Magnetic Nanoparticles

Size-Dependent Magnetic Properties of Colloidal Mn_3O_4 and MnO Nanoparticles**

*Won Seok Seo, Hyong Hoon Jo, Kwangyeol Lee, Bongsoo Kim, Sang Jun Oh, and Joon T. Park**

Metal-oxide nanocrystals are expected to find useful applications in catalysis, energy storage, magnetic data storage, sensors, and ferrofluids.[1] In particular, colloidal metal-oxide nanocrystals are of great interest for technological applications owing to their unique size-dependent properties and excellent processability. Recent advances in the colloidal synthesis of metal oxides reveal that thermal decomposition of metal acetylacetonates,[2] metal cupferronates,[3] metal alkoxides,[4] and metal carbonyls[5] in complex organic solvent systems can lead to monodisperse metal oxide nanoparticles in certain cases.

Manganese oxides are widely used as electrode materials,[6] catalysts,[7] and soft magnetic materials.[8] In spite of their important applications, there has been only one report on synthesis of monodisperse colloidal manganese-oxide nanoparticles.[3] Furthermore, a systematic study on the relationship between particle size and physical properties has never been conducted. Herein we report a simple, reliable synthesis of size-focused colloidal nanocrystals of two different manganese oxides, Mn_3O_4 and MnO, from thermal decomposition of a single precursor $[Mn(acac)_2]$ (acac = acetylacetonate) in oleylamine, as well as their unique size-dependent magnetic properties.

A slurry of $[Mn(acac)_2]$ (0.3 g) in oleylamine (7.6 g; 1:24 molar ratio) was heated at 180 °C for 9 h under an atmosphere of argon, and the resulting reaction mixture was cooled to room temperature to form a brown suspension. After centrifugation at 3000 rpm for 10 min, the supernatant was removed to afford a brown precipitate. Dichloromethane (10 mL) was added to the resulting brown precipitate to give a brown suspension, which was sonicated for 10 min to form a clear solution. Removal of the insoluble material, if any, by centrifugation and precipitation by adding ethanol (40 mL) produced a brown powder, which could be easily redispersed in various organic solvents such as hexane, toluene, and dichloromethane. The low-resolution transmission-electron-microscope (TEM) image of the powder shows nearly monodisperse spherical nanoparticles of 10 nm in diameter as shown in Figure 1a, and its high resolution TEM image in Figure 1b reveals the highly crystalline nature of Mn_3O_4

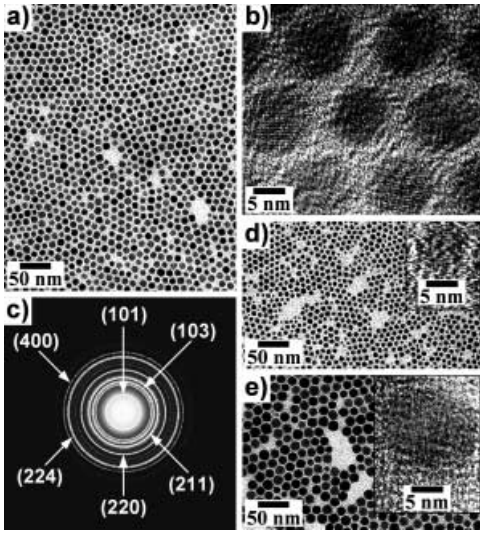

Figure 1. TEM micrographs of Mn_3O_4 nanoparticles: a) TEM image, b) high resolution TEM image, and c) an SAED pattern of 10 nm ($\sigma = 1.0$) nanoparticles. TEM images of d) 6 nm ($\sigma = 0.9$) and e) 15 nm ($\sigma = 1.2$) nanoparticles. High resolution TEM images are shown in the insets.

[*] W. S. Seo, H. H. Jo, Prof. B. Kim, Prof. J. T. Park
National Research Laboratory
Department of Chemistry and School of Molecular Science (BK 21)
Korea Advanced Institute of Science and Technology
Daejeon, 305-701 (Korea)
Fax: (+82) 42-869-5826
E-mail: joontpark@kaist.ac.kr
Prof. K. Lee
Department of Chemistry
Korea University
Seoul, 136-701 (Korea)
Dr. S. J. Oh
Korea Basic Science Institute
Daejeon, 305-333 (Korea)

[**] This research was financially supported by National Research Laboratory (NRL) Program of the Korean Ministry of Science & Technology (MOST), the Korea Science & Engineering Foundation (Project No. 1999-1-122-001-5) for J.T.P, and a Korea University Grant for K.L. We thank staffs of KBSI and KAIST for TEM analyses. We also thank Prof. S. A. Majetich at Carnegie Mellon Univ. for helpful comments.

Supporting information for this article is available on the WWW under http://www.angewandte.org or from the author.

 DOI: 10.1002/ange.200352400

nanoparticles. The selected-area electron-diffraction pattern (SAED) of the nanoparticles is consistent with tetragonal Mn_3O_4 (JCPDS card No.: 24-0734) with strong ring patterns due to (101), (103), (211), (220), (224), and (400) planes (Figure 1c; see Supporting Information for the X-ray diffraction pattern (XRD)). The particle size can be varied easily by a simple change in the reaction temperatures (see Supporting Information for experimental details); smaller nanoparticles of 6 nm in diameter were obtained at 150 °C (Figure 1d) and larger nanoparticles of 15 nm in diameter were prepared at 250 °C (Figure 1e). Although the mechanism leading to Mn_3O_4 and the accompanied oxidation of Mn^{II} to Mn^{III} ions under the employed reaction conditions is not clear at the moment, the oxygen in nanoparticles should originate from the decomposition of acetylacetonate ligand in the $[Mn(acac)_2]$ precursor because the reaction has been conducted with rigorous exclusion of other oxygen sources. Several metal oxides have been prepared by thermal decomposition of metal acetylacetonates under an inert atmosphere,[2a,9] and it has been proposed that carbon dioxide acts as the main oxidant among the various products from ligand decomposition.[9b]

A dramatic change in the decomposition behavior of the precursor $[Mn(acac)_2]$ was observed when 10 equiv of water was introduced to the reaction slurry of $[Mn(acac)_2]$ in oleylamine (1:24 molar ratio). Only pure cubic MnO (JCPDS card No.: 07–0230) was obtained without contamination by Mn_3O_4 (see Supporting Information for the XRD pattern). The presence of water prohibits further oxidation of the formed MnO, presumably because the water is involved in the decomposition of the acetylacetonate ligand, which acts as the oxygen source. Again a simple change in the reaction temperatures results in variation of the MnO nanoparticle size as shown in Figure 2 (see Supporting Information for experimental details): 11 nm particles (220 °C, 9 h), 17 nm particles (220 °C, 3 h and then 250 °C, 6 h), and 22 nm particles (250 °C, 9 h).

Size-dependent magnetic properties of the Mn_3O_4 nanoparticles of varying sizes were studied by using a superconducting quantum interference device (SQUID). As expected, the three Mn_3O_4 nanoparticle samples showed ferromagnetic behaviors at low temperatures, whereas they were paramagnetic at room temperature.[10] Under zero-field-cooling (ZFC) measurements at 100 Oe, the observed blocking temperatures T_B were 36 K, 40 K, and 41 K for 6 nm, 10 nm, and 15 nm Mn_3O_4 nanoparticles, respectively, as shown in Figure 3. This result is consistent with the linear relationship between crystal volume V and blocking temperature T_B as predicted from the equation $KV = 25 k_B T_B$ (K is the anisotropy constant and k_B is Boltzmann's constant;[11] a similar trend was also observed for other ferromagnetic materials such as Co[12] and Fe_2O_3 nanoparticles.[5]

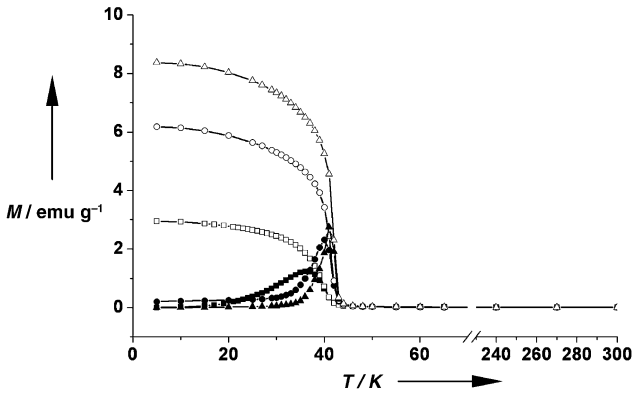

Figure 3. ZFC (filled symbols) and FC (open symbols) magnetization curves of 6 nm (squares), 10 nm (circles), and 15 nm (triangles) Mn_3O_4 nanoparticles under an applied field of 100 Oe.

It has been recently reported that very small MnO nanoparticles (5–10 nm in diameter) show weak ferromagnetic behavior at low temperatures,[13] although bulk MnO shows antiferromagnetic behavior with $T_N \approx 125$ K. The observed weak ferromagnetism has been ascribed to the presence of noncompensated surface spins on the antiferromagnetic core of the MnO nanoparticle.[13] Measurements of size-dependent magnetism, however, have never been reported for MnO nanoparticles. The three MnO samples showed the expected weak ferromagnetic behavior at low temperatures, but unusual size-dependency of magnetic properties was observed for MnO nanoparticles. Under ZFC measurements at 100 Oe, the observed blocking temperatures T_B were 25 K, 18 K, and 10 K for 11 nm, 17 nm, and 22 nm MnO nanoparticles, respectively (Figure 4). This result is, to the best of our knowledge, the first demonstration of an inverse proportionality of the blocking temperature to the particle size. It is likely that smaller MnO nanoparticles with higher surface-to-volume ratio exhibit much larger proportion of noncompensated surface spins on the antiferromagnetic core and thus reveal higher T_B and magnetization values than those of larger nanoparticles.

In summary, we have prepared soluble, highly crystalline, monodisperse, and size-controlled Mn_3O_4 and MnO nanoparticles by thermal decomposition of a single precursor $[Mn(acac)_2]$ in oleylamine under an inert atmosphere, and have demonstrated their unique size-dependent magnetic properties. The particle size can be easily manipulated by

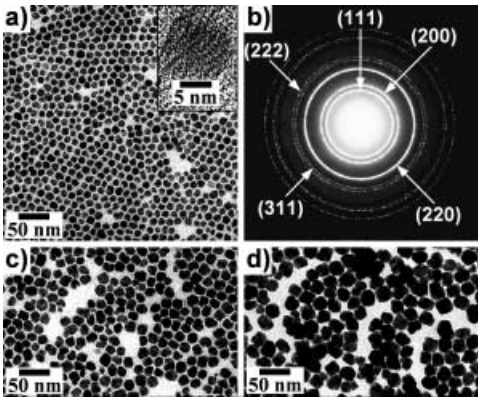

Figure 2. TEM micrographs of MnO nanoparticles: a) TEM image and b) a SAED pattern of 11 nm ($\sigma = 1.1$) nanoparticles. High resolution TEM image is in the inset. TEM images of c) 17 nm ($\sigma = 1.6$) and d) 22 nm ($\sigma = 2.3$) nanoparticles.

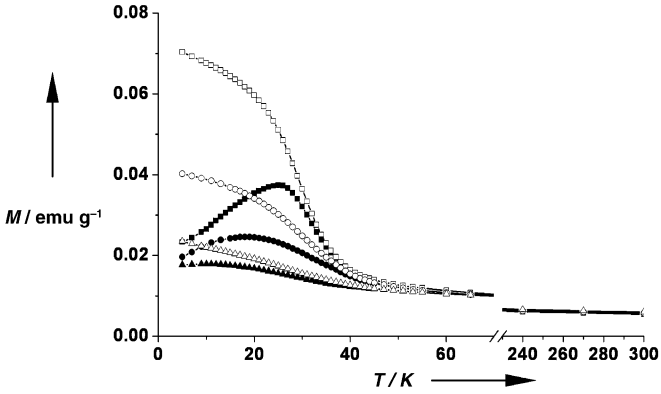

Figure 4. ZFC (filled symbols) and FC (open symbols) magnetization curves of 11 nm (squares), 17 nm (circles), and 22 nm (triangles) MnO nanoparticles under an applied field of 100 Oe.

simply changing the employed reaction temperature, and moreover the metal-oxide phase was effectively controlled by the presence or absence of a small amount of water. Detailed magnetic property measurements and theoretical calculations for the observed unusual magnetic behavior are underway for the prepared manganese oxide nanoparticles.

Experimental Section

Syntheses of MnO and Mn_3O_4 nanoparticles: See Supporting Information.

Characterization: The prepared nanoparticles were characterized by XRD (Rigaku D/MAX-RB (12 kW) diffractometer with a graphite-monochromatized $Cu_{K\alpha}$ radiation source at 40 kV and 120 mA), TEM (low resolution: Omega EM912 operated at 120 kV; high resolution: Philips F20Tecnai operated at 200 kV), selected area electron diffraction (SAED) patterns attached to EM912, and energy dispersive analyses of X-ray emission (EDAX) attached to EM912. Samples for TEM investigations were prepared by putting an aliquot of dichloromethane solution of nanoparticles onto an amorphous carbon substrate supported on a copper grid. The excess liquid was then removed with tissue, and the grid was allowed to dry at room temperature. Magnetic measurements were performed on a SQUID magnetometer (Quantum Design MPMS-7). DC susceptibility and hysteresis measurements were recorded for powdered samples of nanoparticles in a gelatin capsule. The temperature was varied between 5 and 300 K according to a zero-field-cooling/field-cooling (ZFC/FC) procedure at 100 Oe, and the hysteretic loops were obtained in a magnetic field that varied from +7 to −7 T.

Received: July 17, 2003
Revised: November 11, 2003 [Z52400]

Keywords: colloids · magnetic properties · manganese · nanoparticles

[1] a) A. J. Zarur, J. Y. Ying, *Nature* **2000**, *403*, 65–67; b) S. A. Majetich, Y. Jin, *Science* **1999**, *284*, 470–473; c) C. Nayral, E. Viala, P. Fau, F. Senocq, J.-C. Jumas, A. Maisonnat, B. Chaudret, *Chem. Eur. J.* **2000**, *6*, 4082–4090; d) K. Raj, R. Moskowitz, *J. Magn. Magn. Mater.* **1990**, *85*, 233–245.

[2] a) W. S. Seo, H. H. Jo, K. Lee, J. T. Park, *Adv. Mater.* **2003**, *15*, 795–797; b) S. Sun, H. Zeng, *J. Am. Chem. Soc.* **2002**, *124*, 8204–8205.

[3] J. Rockenburger, H. C. Scher, A. P. Alivisatos, *J. Am. Chem. Soc.* **1999**, *121*, 11595–11596.

[4] S. O'Brien, L. Brus, C. B. Murray, *J. Am. Chem. Soc.* **2001**, *123*, 12085–12086.

[5] T. Hyeon, S. S. Lee, J. Park, Y. Chung, H. B. Na, *J. Am. Chem. Soc.* **2001**, *123*, 12798–12801.

[6] a) J. C. Nardi, *J. Electrochem. Soc.* **1985**, *132*, 1787–1790; b) A. R. Armstrong, P. G. Bruce, *Nature* **1996**, *381*, 499–500.

[7] a) L. Hegedus, J. W. Beckman, W. H. Pan, J. P. Solor, Eur. Pat. Appl. 345,695, **1989**; b) M. Baldi, E. Finocchio, F. Milella, G. Busca, *Appl. Catal. B* **1998**, *16*, 43–51.

[8] Chugai Electric Industrial Co. Ltd., Japan Pat. Appl. 82,209,833, **1982**.

[9] a) L. A. Ryabova, V. S. Salun, L. A. Serbinov, *Thin Solid Films* **1982**, *92*, 327–332; b) A. G. Nasibulin, P. P. Ahonen, O. Richard, E. I. Kauppinen, I. S. Altman, *J. Nanopart. Res.* **2001**, *3*, 385–400.

[10] K. Dwight, N. Menyuk, *Phys. Rev.* **1960**, *119*, 1470–1479.

[11] C. P. Bean, J. D. Livingston, *J. Appl. Phys.* **1959**, *30*, 120S-129S.

[12] J.-I. Park, N.-J. Kang, Y.-W. Jun, S. J. Oh, H.-C. Ri, J. Cheon, *ChemPhysChem* **2002**, *3*, 543–547.

[13] G. H. Lee, S. H. Huh, J. W. Jeong, B. J. Choi, S. H. Kim, H.-C. Ri, *J. Am. Chem. Soc.* **2002**, *124*, 12094–12095.

